

# HENRY

Hydraulic Engineering Repository

Ein Service der Bundesanstalt für Wasserbau

---

Conference Paper, Published Version

**Bollaert, Erik F. R.; Hofland, Bas**

## **The Influence of Flow Turbulence on Particle Movement due to Jet Impingement**

---

Verfügbar unter/Available at: <https://hdl.handle.net/20.500.11970/99941>

Vorgeschlagene Zitierweise/Suggested citation:

Bollaert, Erik F. R.; Hofland, Bas (2004): The Influence of Flow Turbulence on Particle Movement due to Jet Impingement. In: Chiew, Yee-Meng; Lim, Siow-Yong; Cheng, Nian-Sheng (Hg.): Proceedings 2nd International Conference on Scour and Erosion (ICSE-2). November 14.–17., 2004, Singapore. Singapore: Nanyang Technological University.

### **Standardnutzungsbedingungen/Terms of Use:**

Die Dokumente in HENRY stehen unter der Creative Commons Lizenz CC BY 4.0, sofern keine abweichenden Nutzungsbedingungen getroffen wurden. Damit ist sowohl die kommerzielle Nutzung als auch das Teilen, die Weiterbearbeitung und Speicherung erlaubt. Das Verwenden und das Bearbeiten stehen unter der Bedingung der Namensnennung. Im Einzelfall kann eine restriktivere Lizenz gelten; dann gelten abweichend von den obigen Nutzungsbedingungen die in der dort genannten Lizenz gewährten Nutzungsrechte.

Documents in HENRY are made available under the Creative Commons License CC BY 4.0, if no other license is applicable. Under CC BY 4.0 commercial use and sharing, remixing, transforming, and building upon the material of the work is permitted. In some cases a different, more restrictive license may apply; if applicable the terms of the restrictive license will be binding.



# THE INFLUENCE OF FLOW TURBULENCE ON PARTICLE MOVEMENT DUE TO JET IMPINGEMENT

ERIK BOLLAERT

*AquaVision Engineering Ltd., PO BOX 73 EPFL,  
CH-1015 Lausanne, Switzerland*

BAS HOFLAND

*Fluid Mechanics Section (Laboratory), Faculty of Civil Engineering and Geosciences,  
Delft University of Technology, PO BOX 5048, 2600 GA Delft, The Netherlands*

Particle movement in granular river beds or rocky plunge pools is traditionally assessed based on shear stress. However, this approach neglects possible influences of flow turbulence on the forces that move the particle. Force fluctuations are generally generated by two means: quasi-steady fluctuations of the mean velocity, which influence drag and lift forces, and localized turbulent pressures near the particle, caused by pressure gradients near the solid boundary. The former fluctuations are highly dependent on the relative particle protrusion, while the latter fluctuations remain even for no protrusion. In the following, two series of experiments with impinging jets are presented: the first tests are relevant to movement of rock blocks without protrusion, while the second tests describe entrainment of granular riverbed particles with protrusion.

## 1 Introduction

Movement of rock blocks in plunge pools or granular material in riverbeds may result in significant erosion problems near hydraulic structures. Examples are scour of rock downstream of large dams or scour of bridge piers. Scour and erosion of granular material are generally assessed based on shear stress or stream power approaches. The former approach considers the fluid forces parallel to the particle boundary to express entrainment. It indirectly also accounts for lift forces by means of an experimentally calibrated entrainment coefficient. The latter approach considers the rate of energy dissipation or the work performed by the flow, which accounts for all possible forms of energy losses in the whole flow volume and not only close to the particles.

Most investigations result in contradictory statements regarding the relative importance of drag and lift forces on particle entrainment. The critical shear stress is a value difficult to define and subject to stochastic modeling. Moreover, particle stability exponentially depends on its protrusion (Fenton & Abbott, 1977; Coleman et al., 2003), which is difficult to determine. Furthermore, flow turbulence is most often discarded from the analysis or dealt with in a simplified manner. Breusers (1967) accounted for turbulence by means of a local turbulence coefficient, which considers the ratio of standard deviation of instantaneous velocity over time-averaged velocity. Experimentally derived values of the local turbulence coefficient as well as corresponding scour formulas are proposed in Hoffmans & Verheij (1997) for a large range of hydraulic structures. Bollaert (2002, 2004) recently developed a model for rock block entrainment based on the ability of an impinging jet to create pressure fluctuations at a plunge pool bottom. The erosive capacity of the flow is expressed by the RMS values of the pressure

fluctuations at the bottom, which have been measured on a near-prototype experimental facility. These values are then used in an erosion resistance model. No influence of bottom shape or particle roughness or protrusion is considered however.

None of the existing approaches considers the mechanics of turbulence in detail. Especially the relationship between the instantaneous velocity and pressure fields and the resulting net forces on a particle are not fully understood. For this, a more detailed assessment of turbulent coherent structures in the vicinity of the particle, as well as the forces they may generate, is necessary. This assessment has lastly been performed for large stones on rough river beds (Hofland et al., 2004) and is now being extended towards movement of rock blocks due to jet impact in plunge pools.

The present paper describes two series of experiments with jets impinging on bottom particles. The first series of experiments have been performed at the Swiss Federal Institute of Technology in Lausanne, Switzerland, and concern vertical jet impingement on a modeled rock block. For a range of jet velocities and plunge pool water depths, the fluctuating pressures have been measured simultaneously at the upper side and the underside of the modeled block. This allowed expressing the maximum net uplift force on the block as a function of time and turbulent pressures.

Second, a series of tests have been performed at Delft University of Technology, The Netherlands. The tests deal with oblique jet impingement onto a granular riverbed and have been performed for different degrees of jet diffusion and particle protrusion. Flow velocities and pressure fluctuations around the particle were measured simultaneously. The flow velocity field has been measured by means of a PIV technique, while the pressures were recorded by miniature pressure sensors. Moreover, the particle was able to rotate around its downstream axis following a sudden pressure pulse and to bounce back on its original position. Hence, particle movement has been recorded as a function of protrusion and flow turbulence.

## **2 Mechanisms of particle entrainment**

Two different kinds of turbulence-induced forces are relevant. The first kind of forces represents the fluctuating drag and lift forces, which are induced by low-frequency quasi-steady flow fluctuations. These forces are thus generated by the same process that causes the mean forces and mainly depend on the longitudinal velocity. The second kind of forces is induced by fluctuating turbulent pressures at the water-particle interface. They result from pressure gradients, which are inherent to a turbulent flow field, especially in case of protruding particles.

Which of these forces is predominant largely depends on the characteristics of the bottom and the position of the particle compared to its surroundings (= relative protrusion). Other parameters of influence are angle of repose, imbrication, shielding, shape, etc. This is depicted in Figure 1.

The left hand side presents a perfectly flat and smooth bottom, such as described in § 3. No significant drag and lift forces are generated by the quasi-steady flow mechanisms. Only turbulent pressure fluctuations are able to dislodge the particle, as has been proved by the experiments in § 3. The right hand side presents a very rough bottom with highly protruding particles. For such a configuration, the quasi-steady forces generate drag and related lift forces that are largely predominant for protruding particles. For shielded particles, turbulent pressures may play a role.

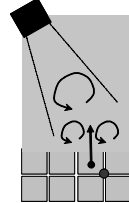

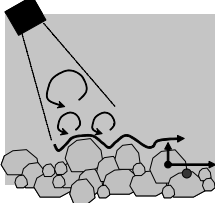



Type of bottom			
Type of entrainment			
Predominant forces	Turbulent pressures	Turbulent pressures Drag and lift forces	Drag and lift forces

Figure 1. Main mechanisms of particle entrainment as a function of type of water-particle interface.

Finally, the midside configuration presents a typical granular riverbed where some paving and rearrangement of particles has taken place due to previous flows. The bottom is rough but the particles do not protrude in an extensive manner. Here, both quasi-steady and turbulent forces may play a role.

In the following, experimental results are presented for both the left hand side and middle cases of Figure 1.

### 3 Plunge pool jet impingement

#### 3.1 Experimental installation

The test installation is presented in Figure 2. It consists of a 72 mm diameter vertically impinging jet, a 3 m diameter plunge pool with maximum water depth of 1 m, and a rectangular shaped rock block with a thickness of only 1 mm (2D approach). Pressure fluctuations are simultaneously recorded at two locations over the block surface (positions a and a') and at one location underneath the block (position d). This allows expressing the net uplift forces and impulsions on the block as a function of jet diffusion and turbulence. It has to be noted that, because of the perfectly flat and smooth bottom, these uplift forces are solely due to a transfer of turbulent pressures underneath the block and not due to quasi-steady drag and/or lift forces. The results are presented in Figure 3 and indicate that the turbulent pressure field may generate significant net uplift forces on the rock block.

#### 3.2 Net uplift pressures on rock blocks

The net uplift forces are defined by the so-called net uplift coefficient  $C_p^{up}$ . This coefficient represents the maximum difference between the pressures at sensor (d) and the average value of the pressures at sensors (a) and (a'). This difference is assumed to correspond to the maximum net instantaneous uplift pressure measured on the block.

Beside the values for submerged jets, for which turbulent jet flow differs because no air is entrained, most of the coefficients are situated between 0.8 and 1.6. Actual design criteria consider a  $C_p^{up}$  of 0.5-1.0 as the maximum possible value. Bellin & Fiorotto

(1995) made measurements of net uplift forces on concrete slabs and proposed an absolute maximum value of 0.5. Liu et al. (1998) measured net uplift pressures on simulated rock blocks of 2 to 4 times the root-mean-square value, i.e. uplift coefficients of 0.5 to 1.0.

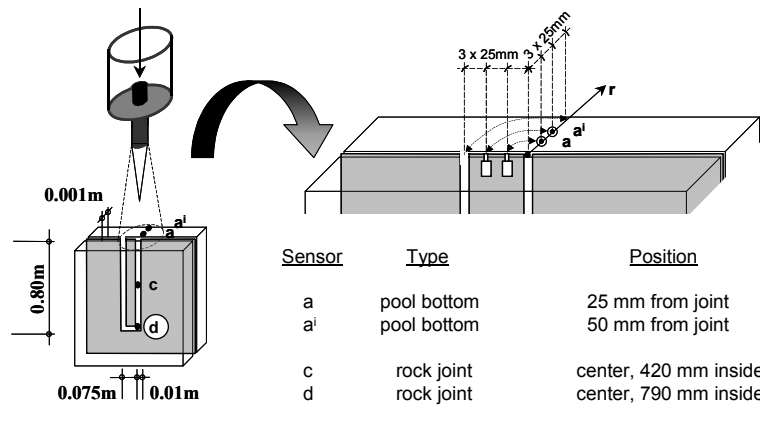


Figure 2. Experimental installation showing vertical plunging jet and modeled rock block. Pressures are recorded at positions a, a' and d.

By applying a maximum underpressure everywhere under the block together with zero pressure at the surface, a physically maximum value of 1.0 is obtained. However, the measured net uplift pressures demonstrate the importance of turbulent pressures at the bottom. Due to turbulence, high pressure pulses underneath may be combined with low pressures at the surface. The size and structure of turbulent eddies compared to the side length of the block thereby plays a significant role.

Figure 3a shows the net uplift coefficient  $C_p^{up}$  as a function of the ratio of plunge pool water depth over jet diameter at impact  $Y/D_j$ . The latter ratio represents the geometrical development of the jet in the water. For values between 6 and 12, flow turbulence attains its maximum possible value, further diffusion of the jet results in a decrease of turbulence. A comparison with the theoretical curve of maximum possible bottom pressure coefficients shows that the net pressure differences over and under the block may become much more significant. This underlines the importance of the turbulent flow structure and fluctuating pressures on the entrainment of the block.

Second, Figure 3b presents the net uplift coefficient as a function of jet velocity at impact  $V_j$ . The coefficients for submerged jets are substantially lower than the ones for aerated impinging jets. This is due to the presence of air in the joint underneath the rock block, which slows down the pressure transfer speed (wave speed) and thus completely modifies the correlation between the under pressures and the surface pressures.

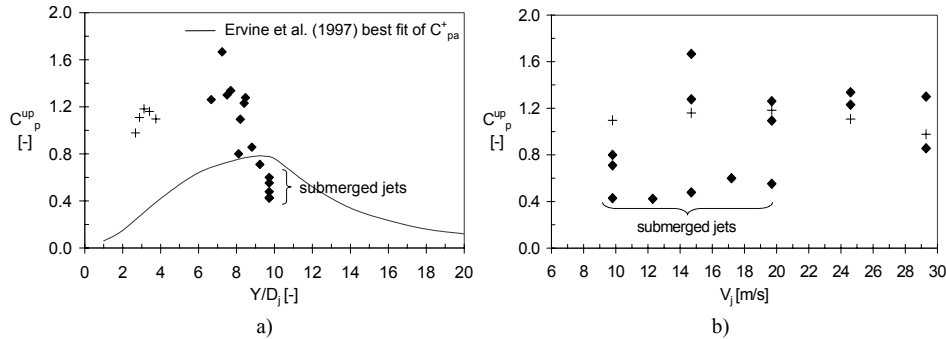


Figure 3. Net uplift pressure coefficients  $C_p^{up}$ : a)  $C_p^{up}$  as a function of  $Y/D_j$ ; b)  $C_p^{up}$  as a function of  $V_j$ .

## 4 Granular riverbed jet impingement

### 4.1 Experimental installation

A second series of tests has been performed with oblique impinging jets on a granular riverbed. The size of the granular particles was in the range of half of the jet diameter upon impact, which means that the particles may be considered as rock blocks in plunge pools. These tests aim at a better assessment of the mechanisms of block entrainment under turbulent flow impact. A range of turbulent flow situations has been tested, some of which are described in a companion paper by Booij & Hofland (2004).

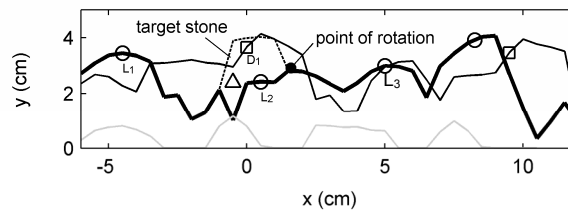


Figure 4. Measured longitudinal sections of the granular bed indicating positions of pressure sensors (○: upward/lift, □: drag, off-centre) and motion sensor (Δ). Dashed line: target stone, thick line: centre of flume, thin line: 40 mm off-centre, grey line: fixed bed. Flow is from left to right.

Figure 4 illustrates the particle configuration on the river bed. A target particle (dashed line) is able to rotate around a fixed downstream point and is connected with a motion sensor at the upstream side. Four pressure sensors are inserted in the bottom:

- (1) Sensor L1: situated 4.5 cm upstream of the target particle and along the centerline of the channel; membrane pointing upwards.
- (2) Sensor L2: situated directly underneath the target particle, in the middle; membrane pointing upwards.
- (3) Sensor L3: situated 4.5 cm downstream of the target particle and along the centerline of the channel; membrane pointing upwards.
- (4) Sensor D1: situated 4 cm sideward from the target particle; membrane pointing horizontally towards upstream, thus directly exposed to the flow.

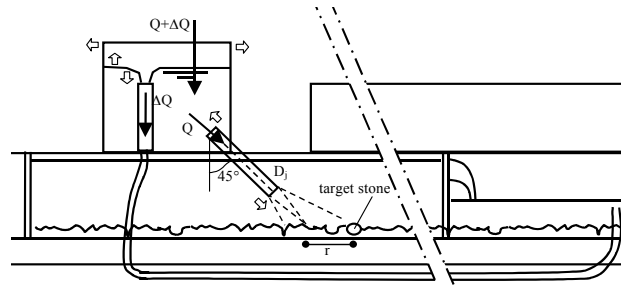


Figure 5. Side view of experimental facility showing the upstream constant head tank, the cylindrical jet and the granular riverbed. Flow is from right to left.

Experiments have been performed for different jet positions and particle protrusions. The distances from the jet outlet to the particle were 4 (core jet), 8 and 10 (developed jets) times the jet diameter (0.053 m). Two particle protrusions have been tested: 6.5 mm and 8.5 mm elevation compared to the average level of the tops of the surrounding particles.

The bed material has a nominal diameter of 17.8 mm. In order to obtain clear entrainment conditions, the target particle has a density of only 1'300 kg/m<sup>3</sup>. The main mode is pivoting. This is obtained by the downstream fixation of the stone, such that free rotating motion remains possible but sliding is avoided.

The equipment consists of a LaVision PIV system to measure the streamwise vertical 2D velocity fields in the centre of the flume above the target particle. The sampling frequency is 15 Hz and the vector spacing 1.2 mm. More details on the PIV set-up and data processing can be found in Hofland & Booij (2004). Miniature low-range piezo-resistive pressure sensors were used to capture the pressure fluctuations.

#### 4.2 *Dynamic pressure fluctuations at riverbed*

The fluctuating pressures have been analyzed statistically and are presented in Figure 6 by means of non-dimensional pressure coefficients. These coefficients represent the measured pressure head (in [m]) divided by the incoming kinetic energy of the jet ( $V^2/2g$ ). Figure 6a shows the mean dynamic pressure coefficients at the riverbed as a function of the lateral distance away from the point of jet impingement ( $r$ ). The parameter  $r_{\max}$  stands for the outer boundary of the turbulent shear layer at the riverbed. For both core and developed jets, good agreement is obtained with exponential curves available in literature and based on previous investigations (Ervine et al. 1997; Bollaert, 2002). Only the values measured under the particle, corresponding to the jet's centerline ( $r = 0$ ), deviate from the curves. This is probably due to the shielding effect of the particle.

Figure 6b presents in a similar manner the fluctuating dynamic pressure coefficients for both core and developed jets. The results are qualitatively similar to the analysis made for the mean dynamic pressures. However, the fluctuations measured under the stone are much closer to theory than the mean values. This would mean that the particle shielding mainly influences the mean pressure rather than the fluctuations.

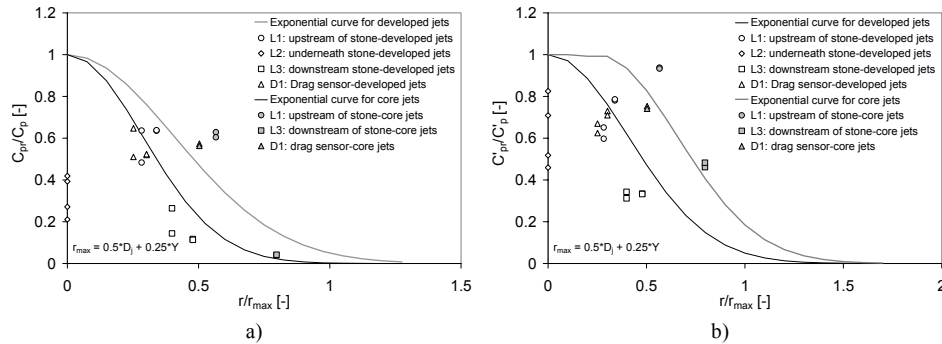


Figure 6. Non-dimensional pressure coefficients as a function of the distance radially outwards from the point of jet impingement ( $r/r_{max}$ ): a) mean dynamic pressures; b) fluctuating dynamic pressures.

As the pressure measurements underneath the stone were affected by the used flexible supply conduit between the point of measurement and the sensor membrane, influencing so a certain range of frequencies of the power spectrum, no sound conclusions can be drawn. The fact that the pressures on protruding particles follow the curves for non-protruding particles is an indication that turbulence pressure gradients are directly causing the forces on the particles, instead of the quasi-steady form drag.

### 4.3 2D instantaneous velocity field at riverbed

The instantaneous 2D velocity field at the moment of a single particle entrainment is presented in Figure 7 for core jet impact. The illustrated velocity stands for measured absolute values minus a constant (reference) convection velocity, in order to better visualize the local turbulence structure.

A large span-wise vortex rotating in the counter-clockwise direction is visible above the particle. This presence of vortices is of significant importance to the generation of net uplift forces on the particle. These are related to RMS fluctuations and constitute a means to describe the importance of turbulence on net uplift forces.

A simplified vortex-model has been developed, in which the vortex is modeled as a single point containing a certain rotation surrounded by potential flow (Hofland et al., 2004). The model points out the relevance of pressures generated by a vortex to particle uplift. For vortices situated straight above the center of the particle, a high pressure on the sides is combined with a low pressure on top of the particle. This may result in large lift forces that can be on the same order of magnitude as the quasi-steady forces, especially in case of vortices with a size close to the particle diameter.

The vortex strength is quantified by the swirling strength  $\lambda$ , which is a measure of the intensity of the local rotation in a flow field.  $\lambda$  is defined as the imaginary part of the complex eigenvalues of the shear tensor. It has a positive value whenever a vortex is present. Figure 7b shows  $\lambda$  for core jets. High swirling strength is obtained just upstream of the center of the particle.



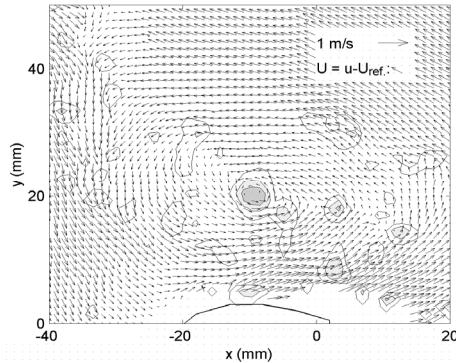


Figure 7.a. 2D instantaneous flow velocity field at moment of particle entrainment. Velocity corresponds to absolute minus convection velocity. The observed vortex has the same size of the particle.

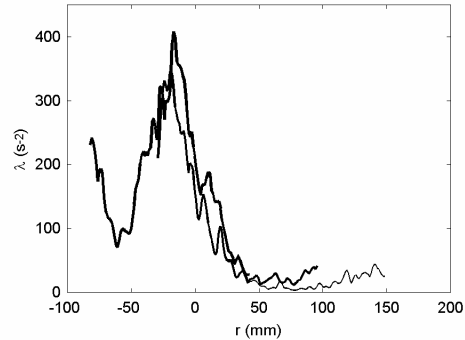


Figure 7.b. Mean swirling strength at  $y=28$  mm as a function of  $r$  for  $Y/D_j = 4$ . A different line represents a different measurement with an altered micro bed topography.

## 5 Conclusions

Particle entrainment due to jet impingement is strongly influenced by turbulent pressure fluctuations at the water-particle interface. This influence increases with decreasing bottom roughness and particle protrusion and may become predominant. Pressure records performed on two independent experimental installations have shown the importance of fluctuating pressures. PIV records of the 2D instantaneous velocity field during particle entrainment point out the presence of vortices that generate large pressure gradients over the particle due to the centrifugal forces. It is believed that turbulent lift forces are directly related to the swirling strength of related vortices close to the particle. Hence, use of swirling strength rather than RMS fluctuations might provide a more profound assessment of particle uplift, especially for highly turbulent flows such as jet impingement in pools.

## References

- Bollaert, E. (2002). "Transient water pressures in joints and formation of scour due to high-velocity jet impact." *Communication 13, EPFL, Switzerland*.
- Bollaert, E. (2004). "A comprehensive model to evaluate scour formation in plunge pools." *Int. J. Hydropower & Dams, 2004*.
- Booij, R., and Hofland, B. (2004). "Measurement of the Mechanisms of Stone Entrainment." *Int. Conference on Scour and Erosion, 2004, Singapore*.
- Breusers, H.N.C. (1967). "Time scale of 2D local scour." *12<sup>th</sup> IAHR Congr., Fort Collins, US*.
- Coleman, S.E., Melville, B.W. and Gore, L. (2003). "Fluvial Entrainment of Protruding Fractured Rock." *J. Hydraulic Eng.*
- Ervine, D.A., Falvey, H.T. and Withers, W. (1997). "Pressure fluctuations on plunge pool floors." *J. Hydraulic Research*.
- Fenton, J.D. and Abbott, J.E. (1977). "Initial movement of grains on a stream bed: The effect of relative protrusion." *Proc. R. Soc. London, Ser. A*.
- Hoffmans, G.J. and Verheij, H.J. (1995). "Scour Manual.", *Balkema, The Netherlands*.
- Hofland, B. and Booij, R. (2004). "Measuring the flow structures that initiate stone movement." *Proc. River Flow 2004, 2<sup>nd</sup> Int. Conf. on Fluvial Hydr., Naples, Italy*.

Hofland, B. Booij, R. Battjes, J.A. (to be published). "Measurement of fluctuating pressures on coarse bed material." *J. Hydraulic Eng.*